



UNIVERSITY OF LEEDS

This is a repository copy of *Spatial Localization of Two Enzymes at Pickering Emulsion Droplet Interfaces for Cascade Reactions*.

White Rose Research Online URL for this paper:

<https://eprints.whiterose.ac.uk/197755/>

Version: Accepted Version

Article:

Li, K, Zou, H, Ettelaie, R orcid.org/0000-0002-6970-4650 et al. (2 more authors) (Cover date: April 3, 2023) *Spatial Localization of Two Enzymes at Pickering Emulsion Droplet Interfaces for Cascade Reactions*. *Angewandte Chemie International Edition*, 62 (15). e202300794. ISSN 1433-7851

<https://doi.org/10.1002/anie.202300794>

© 2023 Wiley-VCH GmbH. This is the peer reviewed version of the following article: Li, K., Zou, H., Ettelaie, R., Zhang, J., Yang, H., *Angew. Chem. Int. Ed.* 2023, 62, e202300794, which has been published in final form at <https://doi.org/10.1002/anie.202300794>. This article may be used for non-commercial purposes in accordance with Wiley Terms and Conditions for Use of Self-Archived Versions. This article may not be enhanced, enriched or otherwise transformed into a derivative work, without express permission from Wiley or by statutory rights under applicable legislation. Copyright notices must not be removed, obscured or modified. The article must be linked to Wiley's version of record on Wiley Online Library and any embedding, framing or otherwise making available the article or pages thereof by third parties from platforms, services and websites other than Wiley Online Library must be prohibited.

Reuse

Items deposited in White Rose Research Online are protected by copyright, with all rights reserved unless indicated otherwise. They may be downloaded and/or printed for private study, or other acts as permitted by national copyright laws. The publisher or other rights holders may allow further reproduction and re-use of the full text version. This is indicated by the licence information on the White Rose Research Online record for the item.

Takedown

If you consider content in White Rose Research Online to be in breach of UK law, please notify us by emailing eprints@whiterose.ac.uk including the URL of the record and the reason for the withdrawal request.



eprints@whiterose.ac.uk
<https://eprints.whiterose.ac.uk/>

Spatial Localization of Two Enzymes at Pickering Emulsion Droplet Interfaces for Cascade Reactions

Ke Li^[a], Houbing Zou^{*[a, b]}, Rammile Ettelaie^[c], Jingxia Zhang^[a] and Hengquan Yang^{*[a, b]}

[a] K. Li, Prof. H. Zou, J. Zhang, Prof. H. Yang
School of Chemistry and Chemical Engineering
Shanxi University
Taiyuan 030006 (China)
E-mail: zouhb@sxu.edu.cn; hqyang@sxu.edu.cn

[b] Prof. H. Zou, Prof. H. Yang
Key Laboratory of Chemical Biology and Molecular Engineering of Ministry of Education, Institute of Molecular Science
Shanxi University
Taiyuan 030006 (China)

[c] Prof. R. Ettelaie
Food Colloids Group, School of Food Science and Nutrition
University of Leeds
Leeds LS2 9JT (UK)

Supporting information for this article is given via a link at the end of the document.

Abstract: Developing biocatalytic cascades in abiological conditions is of utmost significance, but such processes often suffer from low reaction efficiency because of incompatible reaction environments and suppressed intermediate transportation. Here we report a new fashion of biocatalytic cascades by localizing two different enzymes separately in the outer and inner interfacial layers of Pickering emulsion droplets. This versatile approach enables co-location of two enzymes in their preferred reaction microenvironments and simultaneously in nanoscale proximity of each other. The thus-designed interfacial biocatalytic cascades show an outstanding catalytic efficiency in the alkene epoxidation and the thioether oxidation with *in-situ* generation of hydrogen peroxide under mild conditions, 6.9–13.6-times higher than those of the free enzymes in solution and the multi-enzymatic counterparts. Remarkable interfacial effect of Pickering droplets is found to be responsible for the significantly enhanced cascading efficiency.

Introduction

Biocatalytic cascades have increasingly emerged as an advanced synthetic technology for efficient production of fine chemicals because of their noteworthy advantages including exclusive reaction selectivity, simplified intermediate separation and mild reaction conditions.^[1] However, different enzymes with distinctive molecular structures usually require different optimal reaction microenvironments such as the reaction medium, pH value and the reaction temperature.^[2] Accordingly, biocatalytic cascades constructed by simply mixing multiple enzymes in abiological conditions tend to suffer from intractable issues^[1,2], chiefly incompatible reaction conditions, crossed reaction networks and slow intermediate transportation. In this context, ideal biocatalytic cascades in abiotic systems need to tackle two crucial but challenging aspects: (i) spatial isolation of different enzymes within their own preferable reaction microenvironments ensuring reaction networks working effectively and avoiding unwanted mutual interferences; and (ii) localizing different enzymes in intimate close proximity of each other to guarantee efficient molecular transport.

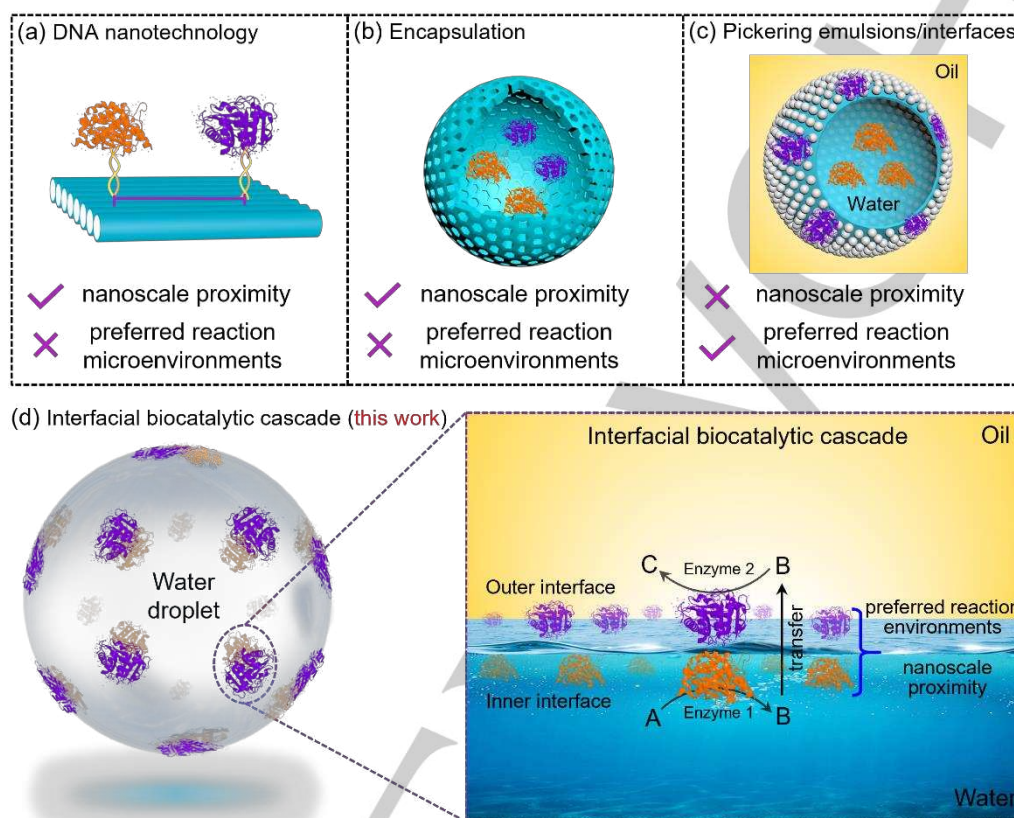
Over the past decade, tremendous research efforts have been devoted to developing various methodologies for biocatalytic cascades.^[3] For instance, DNA nanotechnology was employed to successfully position two different enzymes on a variety of DNA scaffolds (Scheme 1a).^[4] Multiple enzymes were also reported to be encapsulated within various porous materials (Scheme 1b).^[5,6] In comparison to these strategies for the co-immobilization of enzymes, Pickering emulsions that are stabilized by solid particles have advantages in compartmentalizing catalysts within different reaction microenvironments for accelerating cascade reactions because such systems contain two distinct liquid media and thereby provide a versatile platform to assemble multiple catalysts at oil-water interfaces.^[7] For example, MgO-metal and acid-polyoxometalate hybrid catalysts were positioned at Pickering droplet interfaces for biofuel upgrading and adipic acid production,^[8] respectively. Recently, Wu's group arranged one enzyme at Pickering droplet interfaces and another enzyme in the internal water phase via enzyme-polymer conjugates to construct biocatalytic cascades, which showed an enhanced catalytic efficiency compared with the free enzymes in solution.^[9] However, despite the encouraging progresses achieved in accommodating different enzymes in different reaction media,^[9,10] these Pickering emulsion systems were infeasible to precisely control the spatial localization of catalysts in separate but yet very close proximity at droplet interfaces (Scheme 1c). This shortage restricted timely transfer of reaction intermediates from improving cascading efficiency and thus hindered realization of the potential positive interfacial effects for cascade reactions. In this context, there remains a wide gap between these existing biocatalytic cascades and the ideal biocatalytic cascades. Therefore, developing new biocatalytic cascade processes via spatial organization of multiple enzymes in abiotic systems is still an urgent and challenging task.

In this work, we design a system of interfacial biocatalytic cascades for chemical transformations by spatially localizing two different enzymes at the oil-water interfaces of Pickering emulsion droplets. The enzymes were regio-selectively loaded on the hydrophilic or hydrophobic surfaces of Janus mesoporous silica nanosheets (JMSNs) and then were spatially localized in the inner or the outer interfacial layers of Pickering emulsion droplets via an interfacial assembly strategy, respectively. Due to the

RESEARCH ARTICLE

nanoscale thickness of JMSNs, the enzymes isolated in different reaction microenvironments still remained in very close proximity of each other (Scheme 1d). Remarkably, the so designed interfacial biocatalytic cascades showed an outstanding catalytic efficiency in the alkene epoxidation and the thioether oxidation with *in-situ* generation of hydrogen peroxide under mild conditions,

6.9~13.6-fold higher than those of the free enzymes in solution and other multi-enzymatic counterparts. Interfacial effect of Pickering droplets was found to be crucial in avoiding mutual interferences of the enzymatic reaction networks and in facilitating reaction intermediate transportation, thus contributing to the significantly enhanced cascading efficiency.



Scheme 1. Different biocatalytic cascades. (a-c) Biocatalytic cascades constructed via previous strategies: (a) immobilizing multiple enzymes on DNA origami; (b) encapsulating multiple enzymes within porous materials; (c) compartmentalizing enzymes at different regions of Pickering emulsions. (d) Schematic illustration for the interfacial biocatalytic cascades constructed by spatially localizing different enzymes at the interfaces of water droplets.

Results and Discussion

Construction of Interfacial Biocatalytic Cascades

Interfacial biocatalytic cascades were constructed by spatially organizing two different enzymes at the oil-water interfaces of Pickering emulsion droplets via an interfacial localization strategy. Janus mesoporous silica nanosheets ($\text{NH}_2/\text{C}_8/\text{JMSNs}$), with the aminopropyl group ($-\text{NH}_2$) selectively modified on one surface and the octyl groups ($-\text{C}_8$) solely on their other surface, were adopted as the solid emulsifiers because their ordered mesopores were capable of providing fast mass transfer and their distinctive interfacial assembly behavior enabled the spatial localization of various catalysts at Pickering droplet interfaces.^[11] Enzymes with different hydrophilicity/hydrophobicity such as glucose oxidase (GOx) and Lipase B *Candida Antarctica* (CALB) were used to demonstrate the concept of interfacial localization. As illustrated in Figure 1a, GOx was covalently linked to the hydrophilic surface of $\text{NH}_2/\text{C}_8/\text{JMSNs}$ via a Schiff base formation reaction, in which glutaraldehyde served as a linker for attaching GOx with the $-\text{NH}_2$ group. Hydrophobic CALB was then adsorbed on the hydrophobic surface of $\text{NH}_2/\text{C}_8/\text{JMSNs}$ via Van der Waals interactions. In this

way, GOx and CALB were separately immobilized on the opposing hydrophilic and hydrophobic surfaces of $\text{NH}_2/\text{C}_8/\text{JMSNs}$, presenting a dual-enzyme catalyst ($\text{NH}_2\text{-GOx}/\text{C}_8\text{-CALB}/\text{JMSNs}$). Subsequently, the resulting catalyst was employed as a solid emulsifier to produce Pickering emulsions by emulsifying different biphasic oil-water mixtures. Because the two-dimensional JMSNs preferred to parallelly assemble at Pickering droplet interfaces,^[12] GOx loaded on the hydrophilic surface of $\text{NH}_2/\text{C}_8/\text{JMSNs}$ was precisely positioned in the inner interfacial layer of Pickering droplets whereas CALB on their hydrophobic surface was exactly placed in the outer interfacial layer. Meanwhile, the distance between GOx and CALB could be adjusted by altering the thickness of $\text{NH}_2/\text{C}_8/\text{JMSNs}$. On the basis of such an ingenious strategy of interfacial localization, the two different enzymes were not only simultaneously positioned in their preferred reaction media but were also maintained spatially within nanoscale proximity of each other.

$\text{NH}_2/\text{C}_8/\text{JMSNs}$ were prepared according to our previous methods,^[11b,c] and scanning electron microscopy (SEM) images show a morphology of discrete nanosheets with a thickness of nearly 40 nm (Figure S1c). Transmission electron microscopy (TEM) images further showcase that ordered mesochannels were

RESEARCH ARTICLE

perpendicular to the nanosheets (Figure S1g). The asymmetric surface modification was confirmed by Fourier transform infrared (FTIR) spectra and thermogravimetry (TG) analysis as well as Au-NPs labeling experiment (Figure S2). After sequential immobilization of GOx and CALB, the resulting $\text{NH}_2\text{-GOx/C}_8\text{-CALB/JMSNs}$ catalyst still displays a morphology of discrete nanosheets with a thickness of about 40 nm and a uniform mesoporous structure, as is evident in their SEM (Figure 1a) and TEM images (Figure S3). FTIR spectra display the bands of the typical peptide skeleton of enzymes (Figure S4a). Nitrogen sorption analysis indicated that the BET surface area had decreased considerably after loading the enzymes (Figure S4 and Table S1). EDX elemental mapping exhibits the distributions of Si,

C, S, and P element throughout the nanosheets (Figure S3), suggesting the presence of enzymes. To confirm the co-immobilization of the dual enzymes on $\text{NH}_2\text{/C}_8\text{/JMSNs}$, GOx and CALB were separately labeled with Rhodamine B and fluorescein isothiocyanate I (FITC-I) for fluorescence imaging. As depicted in the confocal laser scanning microscopy (CLSM) images, the red fluorescence (Figure 1c) and the green fluorescence (Figure 1d) were observed to homogeneously distribute throughout every nanosheet, and to almost overlap on every nanosheet in the merged fluorescent image (Figure 1e). These results supported that both GOx and CALB have been successfully immobilized on $\text{NH}_2\text{/C}_8\text{/JMSNs}$.

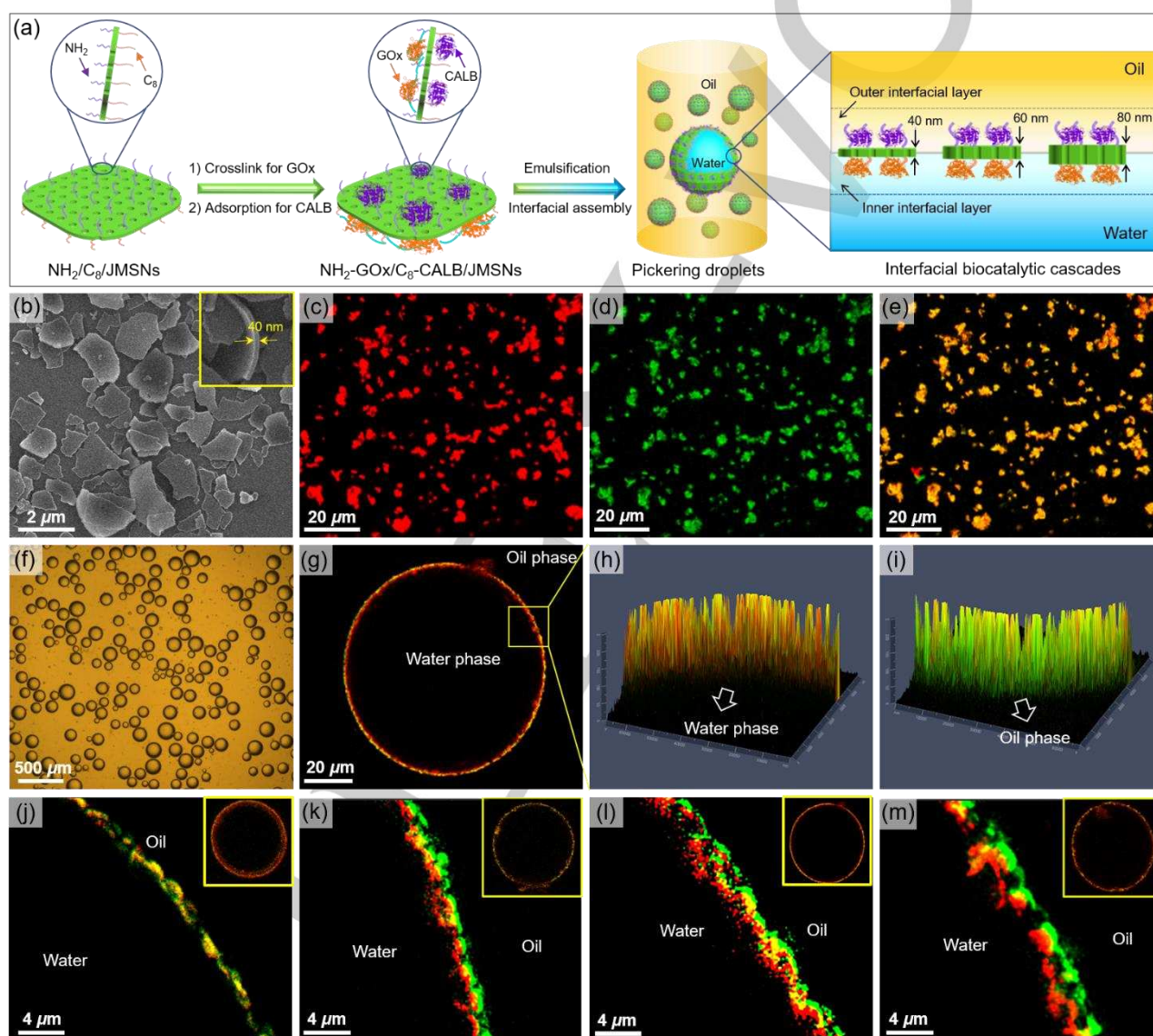


Figure 1. Construction and characterizations of the interfacial biocatalytic cascade. (a) Schematic illustration for the construction of interfacial biocatalytic cascades. (b) SEM image of $\text{NH}_2\text{-GOx/C}_8\text{-CALB/JMSNs}$. (c-e) CLSM images of $\text{NH}_2\text{-GOx/C}_8\text{-CALB/JMSNs}$ in which GOx and CALB were separately labeled with Rhodamine B (c) and FITC-I (d); merged CLSM image (e). (f) Optical micrograph of water-in-oil Pickering emulsions stabilized by $\text{NH}_2\text{-GOx/C}_8\text{-CALB/JMSNs}$. (g) CLSM image of water-in-oil Pickering emulsions stabilized by $\text{NH}_2\text{-GOx/C}_8\text{-CALB/JMSNs}$ in which GOx was labeled with Rhodamine B and CALB was labeled with FITC-I. (h, i) Z-stacked 3D CLSM images of the inner surface (h) and the outer surface (i) of water-in-oil Pickering emulsions stabilized by $\text{NH}_2\text{-GOx/C}_8\text{-CALB/JMSNs}$ in which GOx was labeled with Rhodamine B and CALB was labeled with FITC-I. (j-m) Super-resolution imaging of the oil-water interface of Pickering droplets stabilized by $\text{NH}_2\text{-GOx/C}_8\text{-CALB/JMSNs}$ with different thicknesses in which GOx was labeled with Rhodamine B and CALB was labeled with FITC-I: (j) 40 nm; (k) 60 nm; (l) 70 nm; (m) 80 nm. The inset in b shows the cross-sectional SEM image. The inset in j-m show the corresponding CLSM images.

Because of the asymmetric surface wettability, the $\text{NH}_2\text{-GOx/C}_8\text{-CALB/JMSNs}$ catalyst had a good interfacial activity to produce stable Pickering emulsions. As Figure 1f shows, Pickering emulsions with a droplet size of $100\sim 200\ \mu\text{m}$ were obtained by vigorously stirring a mixture of toluene, water and $\text{NH}_2\text{-GOx/C}_8\text{-CALB/JMSNs}$. By fluorescence dyeing of the water and oil phase, the formed emulsions were ascertained to be water-in-oil type (Figure S5). To inspect the assembly behavior of $\text{NH}_2\text{-GOx/C}_8\text{-CALB/JMSNs}$ at the Pickering droplet interfaces, divinylbenzene containing initiator (benzoyl peroxide) was then used as the oil phase to obtain oil-in-water Pickering emulsions which could be solidified by polymerization for further SEM observations.^[12c] Such SEM images highlight that the droplet size of Pickering emulsions did not change after solidification, but more importantly that the nanosheets were indeed orientated parallel to the surfaces of solidified Pickering droplets (Figure S6). These observations provided direct evidence that the $\text{NH}_2\text{-GOx/C}_8\text{-CALB/JMSNs}$ catalyst was assembled at the droplet interfaces in a parallelly flattening manner. This combination of the unique interfacial assembly pattern and the spatial localization of the two enzymes on $\text{NH}_2\text{/C}_8\text{/JMSNs}$ suggested that GOx and CALB would be desirably positioned in the inner and outer interfacial layers of Pickering droplets, respectively. To validate this suggestion, GOx and CALB were separately labeled with Rhodamine B and FITC-I for fluorescence imaging of their spatial distribution at the Pickering droplet interfaces. CLSM image displays that both red and green fluorescent rings were present around the formed Pickering droplets (Figure 1g). Furthermore, Z-stacked 3D CLSM images clearly exhibit that the red fluorescence appeared on the inner surface of the water droplet (facing the inner water phase, Figure 1h) whereas the green fluorescence was situated on its outer surface (facing the outer oil phase, Figure 1i), thus confirming the spatial distribution of these two different enzymes at the Pickering droplet interfaces.

Furthermore, super-resolution imaging was used to verify the spatial distance between GOx and CALB at the Pickering droplet interfaces. Both GOx and CALB were loaded on $\text{NH}_2\text{/C}_8\text{/JMSNs}$ with different thicknesses ($40\sim 80\ \text{nm}$) by the same immobilization method, which were prepared by adjusting the dosage of tetraethyl orthosilicate (TEOS) during the synthetic procedure (Figure S7). After forming Pickering emulsions (Figure S8), CLSM images reveal that both GOx and CALB located at the oil-water interfaces of Pickering droplets stabilized by $\text{NH}_2\text{-GOx/C}_8\text{-CALB/JMSNs}$ with different thicknesses (the insets in Figures 1j-m). Super-resolution imaging of the Pickering droplet interfaces further exhibits that the red and green fluorescence appeared separately on the interfacial inner and outer surface, once the thickness of JMSNs was increased beyond $60\ \text{nm}$ (Figures 1k-m). Such a segregated fluorescence distribution was not seen at the droplet interfaces when Pickering emulsions were stabilized by $\text{NH}_2\text{-GOx/C}_8\text{-CALB/JMSNs}$ with a thickness of $40\ \text{nm}$ (Figure 1j). This is likely due to the limited spatial resolution of fluorescence imaging.^[5c] Moreover, it is clearly observed that the outer green fluorescence appeared increasingly further away from the inner red fluorescence along with an increase in the $\text{NH}_2\text{/C}_8\text{/JMSNs}$ thickness, giving verification of the controllable proximity between different enzymes in nanoscale level at the Pickering droplet interfaces. Collectively, we have successfully positioned two different enzymes in separate distinct reaction media while simultaneously maintained them in a nanoscale proximity via an exquisite strategy of interfacial localization.

Enhanced Biocatalytic Cascade Reactions

Coupling GOx with CALB is a promising biocatalytic pathway for selective alkene epoxidations by the *in-situ* produced H_2O_2 under mild reaction conditions. However, CALB requires a hydrophobic reaction microenvironment to provide good affinity to organic reactants (alkenes)^[13] while GOx often displays a high activity for aerobic oxidation of glucose to yield H_2O_2 in aqueous solutions.^[14] Mass transfer of the *in-situ* produced H_2O_2 from GOx to CALB is also an unresolved challenge. These intractable issues stemmed from the incompatible reaction conditions and the low reaction intermediate transport make it difficult for the GOx/CALB cascade to be applied in the epoxidation of alkenes by the *in-situ* produced H_2O_2 . Here, the above interfacial biocatalytic cascade developed by us was applied to address the challenges in the GOx/CALB cascade reactions. As Figure 2b depicts, GOx transforms glucose and dioxygen to H_2O_2 in the inner interfacial layer (IIL) of Pickering droplets and subsequently the *in-situ* generated H_2O_2 is supplied to CALB located in the outer interfacial layer (OIL) for producing peracid from octanoic acid to initiate the epoxidation reaction.

As displayed in Figure 2c, the GOx/CALB cascade reaction designed at the Pickering droplet interfaces (GOx-IIL/CALB-OIL) presents a high reaction rate with a conversion of 75.4% and an epoxide selectivity of nearly 100% within 10.0 h in the epoxidation of cyclooctene under ambient conditions. In sharp contrast, GOx and CALB with equal dosage in the conventional biphasic system (GOx+CALB-free, Figure 2a) show a conversion of only 15.0% under the same conditions. By dispersing an equal dosage of GOx and CALB in the internal water phase of Pickering droplets stabilized by $\text{NH}_2\text{/C}_8\text{/JMSNs}$ (GOx+CALB-IPD, Figure S9), a conversion of 18.8% was obtained. These results obtained by the free enzymes in bulk water phase remained in good agreement with those reported in previous literatures^[9a] but were much lower than ones achieved by our interfacial GOx-IIL/CALB-OIL cascade. For further comparison, GOx and CALB were co-immobilized on the nanosheets in a randomly mixed fashion (GOx-CALB/MSNs, Figure S10) and then were positioned around the oil-water interfaces of Pickering droplets without regio-selective distribution (GOx+CALB-PDI, Figure S11). It was found that this GOx+CALB-PDI cascade exhibited a conversion less than 10% under identical conditions, which was still much lower than that of the interfacial GOx-IIL/CALB-OIL cascade. According to the reaction kinetics (Figure 2c), the catalytic efficiency (defined as the moles of converted reactants per milligram of enzymes per h) of GOx-IIL/CALB-OIL was calculated to be $1.34\times 10^{-2}\ \text{h}^{-1}$ (Figure 2d), which was 13.6-times higher than that of the GOx+CALB-PDI cascade without special interfacial localization ($0.10\times 10^{-2}\ \text{h}^{-1}$) and 6.9~8.6 times higher than that of the GOx/CALB cascade in bulk water phase ($0.15\sim 0.19\times 10^{-2}\ \text{h}^{-1}$). These observations illustrate that the control of the spatial localization of GOx and CALB at the Pickering droplet interfaces was very vital for achieving the outstanding catalytic efficiency for the alkene epoxidation.

Furthermore, GOx and CALB were immobilized separately on one $\text{NH}_2\text{/C}_8\text{/JMSNs}$ nanosheet and then were introduced into the inner or outer interfacial layers of Pickering droplets via the same interfacial assembly strategy (GOx/IIL+CALB/OIL, Figure S12). Although also realizing the interfacial localization of GOx and CALB, this GOx/IIL+CALB/OIL cascade had larger (microscale) inter-enzyme separation distances because the enzymes were positioned on two individual JMSN nanosheets. Under the same reaction conditions, this GOx/IIL+CALB/OIL cascade presented a conversion of 30.4% (Figure 2c) and a catalytic efficiency of

RESEARCH ARTICLE

$0.46 \times 10^{-2} \text{ h}^{-1}$ (Figure 2d) in the cyclooctene epoxidation. This result was much higher than that achieved by the GOx+CALB-PDI cascade without interfacial localization and the GOx+CALB-free cascade in bulk water phase, further emphasizing the importance of localizing two enzymes at the droplet interfaces in boosting biocatalytic cascades. Nonetheless, the catalytic efficiency of this GOx-IIL+CALB/OIL cascade was still 2.9-fold lower than that of the interfacial GOx-IIL/CALB-OIL cascade, suggesting that the nanoscale inter-enzyme distance was another vital factor for achieving the outstanding cascading efficiency. To confirm this point, the effect of the proximity between GOx and CALB, residing on the Pickering droplet interfaces, on the cascading efficiency was investigated. As depicted in Figure 2e,

when the inter-enzyme distance is increased from 40 nm to 60 nm, there is a noticeable decline in conversion down from 75.4% to 39.8% under the same reaction conditions. The catalytic efficiency is observed to show a 2.4-fold drop, decreasing from an initial value of $1.34 \times 10^{-2} \text{ h}^{-1}$ down to $0.55 \times 10^{-2} \text{ h}^{-1}$ (Figure 2f). Along with an increase in the inter-enzyme distance from 60 nm to 70 nm, the conversion further drops to 28%, now with a 4.3-fold reduction in the catalytic efficiency. These results demonstrated a clear enzyme-enzyme proximity effect of the interfacial GOx-IIL/CALB-OIL cascade. Collectively, the interfacial localization together with nanoscale inter-enzyme distances should be responsible for the significantly enhanced catalytic efficiency of the interfacial GOx-IIL/CALB-OIL cascade.

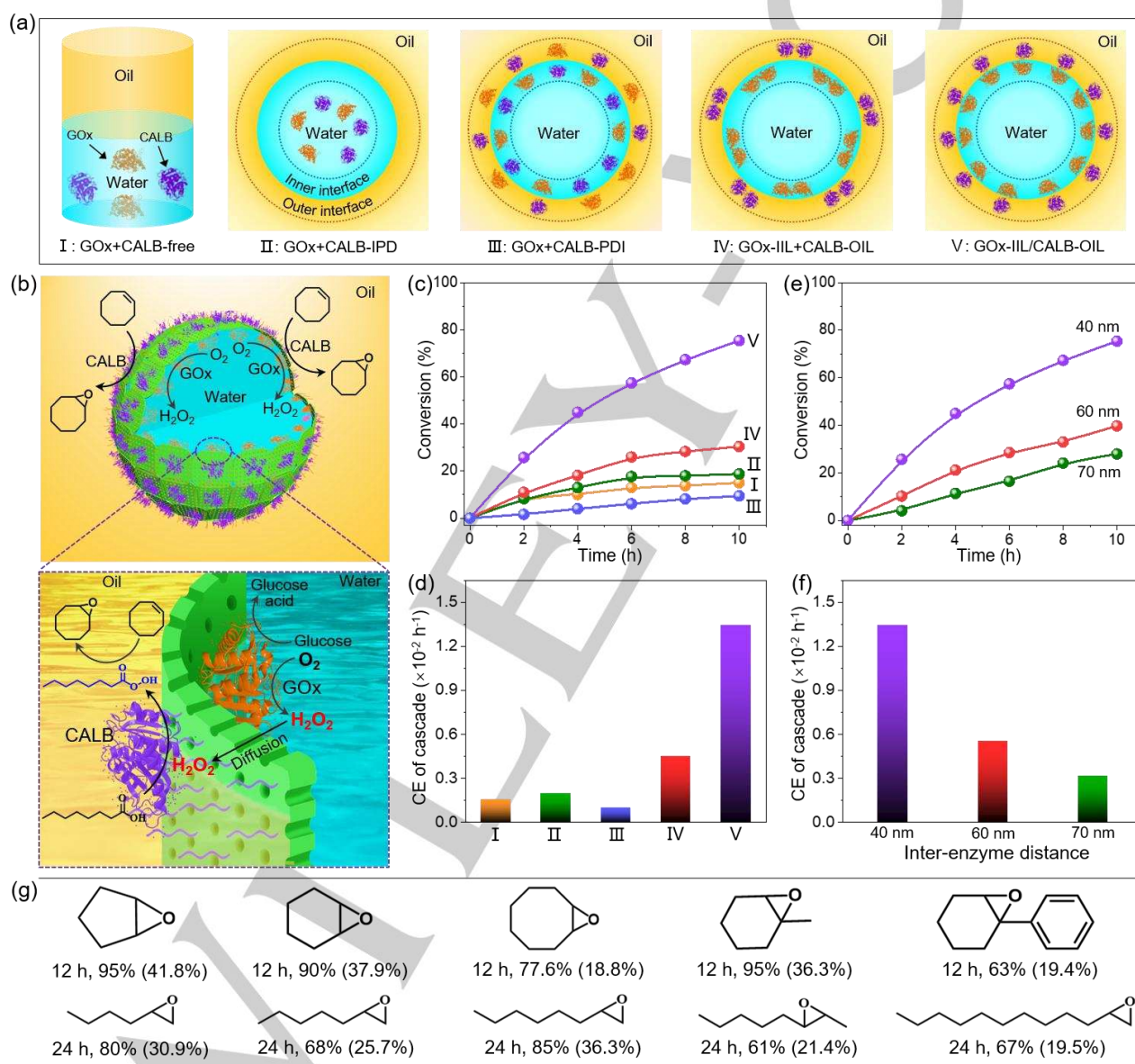


Figure 2. Interfacial biocatalytic cascade for the alkene epoxidations. (a) Schematic illustration for different dual-enzymatic systems including GOx+CALB-free, GOx+CALB-IPD, GOx+CALB-PDI, GOx-IIL+CALB-OIL and GOx-IIL/CALB-OIL. (b) Schematic illustration of the cyclooctene epoxidation reaction catalyzed over the interfacial GOx-IIL/CALB-OIL cascade. (c) Kinetic profiles for the cyclooctene epoxidation with *in-situ* produced H_2O_2 over different dual-enzymatic systems. (d) Catalytic Efficiencies (CE) of different dual-enzymatic systems for the cyclooctene epoxidation. (e) Kinetic profiles for the cyclooctene epoxidation with *in-situ* produced H_2O_2 over the interfacial GOx-IIL/CALB-OIL cascades with different inter-enzyme distances. (f) Catalytic Efficiencies (CE) of the interfacial GOx-IIL/CALB-OIL cascades with different inter-enzyme distances for the cyclooctene epoxidation. (g) Selective epoxidation of various alkenes over the interfacial GOx-IIL/CALB-OIL cascade. Numbers in brackets refer to the results obtained by GOx+CALB-free.

RESEARCH ARTICLE

The interfacial GOx-IIL/CALB-OIL cascade was further applied to the epoxidation of varieties of alkenes under ambient conditions (Figure 2g). Cyclic aliphatic alkenes including cyclopentene, cyclohexene, 1-methylcyclohexene and 1-phenylcyclohexene could all be efficiently converted into their corresponding epoxides with yields of 63%~95% within 12.0 h over the interfacial GOx-IIL/CALB-OIL cascade. For the lineal olefins with different carbon chain lengths that were considered to be difficult to oxidize, the interfacial GOx-IIL/CALB-OIL cascade also exhibited a high yield of 67%~85% within 24.0 h. A good

conversion of 61% was obtained even in the epoxidation of an internal olefin (2-octene). Owing to the mild reaction conditions, the selectivities for epoxides all reached nearly 100%. Importantly, for all these investigated substrates, the conventional free enzymes system (GOx+CALB-free) only exhibited conversions in the range of 18.8%~41.8% under the same conditions. This represented a reduction of 2.3~4.1 times compared with those obtained over the interfacial GOx-IIL/CALB-OIL cascade. These results indicate that our interfacial GOx-IIL/CALB-OIL cascade has a broad substrate scope for alkene epoxidations.

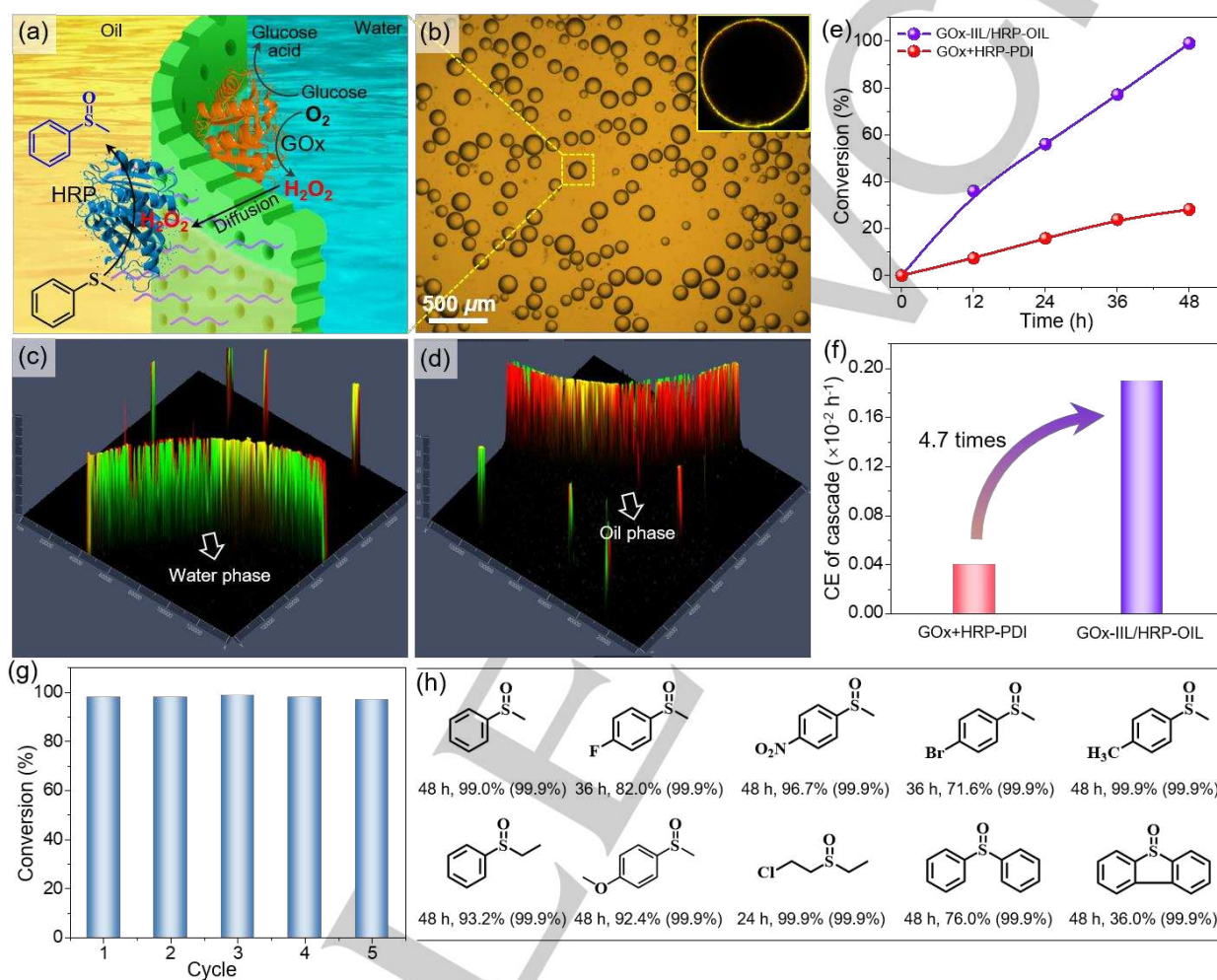


Figure 3. Interfacial biocatalytic cascade for the thioether oxidations. (a) Schematic illustration for the thioether oxidation reaction catalyzed over the interfacial GOx-IIL/HRP-OIL cascade. (b) Optical micrograph of water-in-oil Pickering emulsions stabilized by C_8 -NH₂-HRP/GOx/JMSNs. (c, d) Z-stacked 3D CLSM images of the inner surface (c) and the outer surface (d) of water-in-oil Pickering emulsions stabilized by C_8 -NH₂-HRP/GOx/JMSNs in which GOx was labeled with FITC-I and HRP was labeled with Rhodamine B. (e) Kinetic profiles for the oxidation of phenyl methyl sulfide with *in-situ* produced H₂O₂ over GOx-IIL/HRP-OIL and GOx+HRP-PDI. (f) Catalytic Efficiencies of GOx-IIL/HRP-OIL and GOx+HRP-PDI for the oxidation of phenyl methyl sulfide. (g) Recyclability of the interfacial GOx-IIL/HRP-OIL cascade in the oxidation of phenyl methyl sulfide with *in-situ* produced H₂O₂. (h) Oxidation of various thioethers over the interfacial GOx-IIL/HRP-OIL cascade. Numbers in brackets refer to the selectivity for sulfoxides. The inset in b shows the corresponding CLSM image.

To examine the generality of our interfacial localization strategy, we next explored other multi-enzymatic reactions at the Pickering droplet interfaces. Horseradish peroxidase (HRP) and GOx were regio-selectively immobilized on the hydrophobic and hydrophilic surface of JMSNs (Figure S13) via a Schiff base formation reaction and Van der Waals interactions (see the Experimental Section in the Supporting Information), respectively. After a typical emulsification process, GOx and HRP were precisely positioned in the inner and outer interfacial layers of

Pickering droplets for the thioether oxidations by *in-situ* produced H₂O₂ (Figure 3a). CLSM image in Figure 3b clearly showcase that both HRP and GOx were located at the Pickering droplet interfaces (HRP and GOx were respectively labeled with Rhodamine B and FITC-I). Z-stacked 3D CLSM images further disclose that GOx was in the inner interfacial layer (Figure 3c) while HRP was in the outer interfacial layer (Figure 3d). Interestingly, the obtained interfacial GOx-IIL/HRP-OIL cascade exhibits a nearly full conversion within 48 h in the oxidation of

RESEARCH ARTICLE

phenyl methyl sulfide to phenyl methyl sulfoxide (Figure 3e). In contrast, only a conversion of 23% was obtained under the same reaction conditions when both enzymes distributed randomly at the Pickering droplet interfaces without special spatial localization (GOx+HRP-PDI, Figure S14). According to the reaction kinetics, the catalytic efficiency of interfacial GOx-IIL/HRP-OIL cascade was 4.7-times higher than that of GOx+HRP-PDI (Figure 3f). Meanwhile, the current GOx/HRP system was also applicable to the oxidation of a variety of thioethers. As listed in Figure 3h, the interfacial GOx-IIL/HRP-OIL cascade presents a conversion of 71.6%~99.9% in the oxidation of phenyl methyl sulfides with different substituted groups at the aryl moiety. For the challenging substrates such as diphenyl sulfide and dibenzothiophene that are difficult to oxidize due to the steric hindrance, good conversions of 76% and 36% were obtained under the current mild conditions, respectively. In the oxidation of (2-chloroethyl) ethyl sulfide, an organosulfur CWA (chemical warfare agents) simulant, our interfacial GOx-IIL/HRP-OIL cascade also gave a

superior degradation efficiency with a conversion of 99% within 12 h. Notably, the selectivities for sulfoxides all reached as high as 99.9%. These results demonstrated that spatially localizing two different enzymes at the Pickering droplet interfaces was a general strategy for boosting multi-enzymatic cascade reactions.

Furthermore, the recyclability of the interfacial GOx-IIL/HRP-OIL cascade was investigated. The catalyst was collected from the reaction system via high-speed centrifugating at the end of the reaction and then washed by PBS solution. The recovered catalyst was then used as the solid emulsifier once again to produce Pickering emulsions for the next reaction cycle. As shown in Figure 3g, the interfacial GOx-IIL/HRP-OIL cascade still gives a very high conversion of 97.5% within an extended reaction time (72.0 h) in the oxidation of phenyl methyl sulfide after five reaction cycles. These results suggested a good recyclability, which was likely due to the fact that the enzyme deactivation caused by high concentrations of H₂O₂ has been avoided during the process of interfacial biocatalytic cascades.

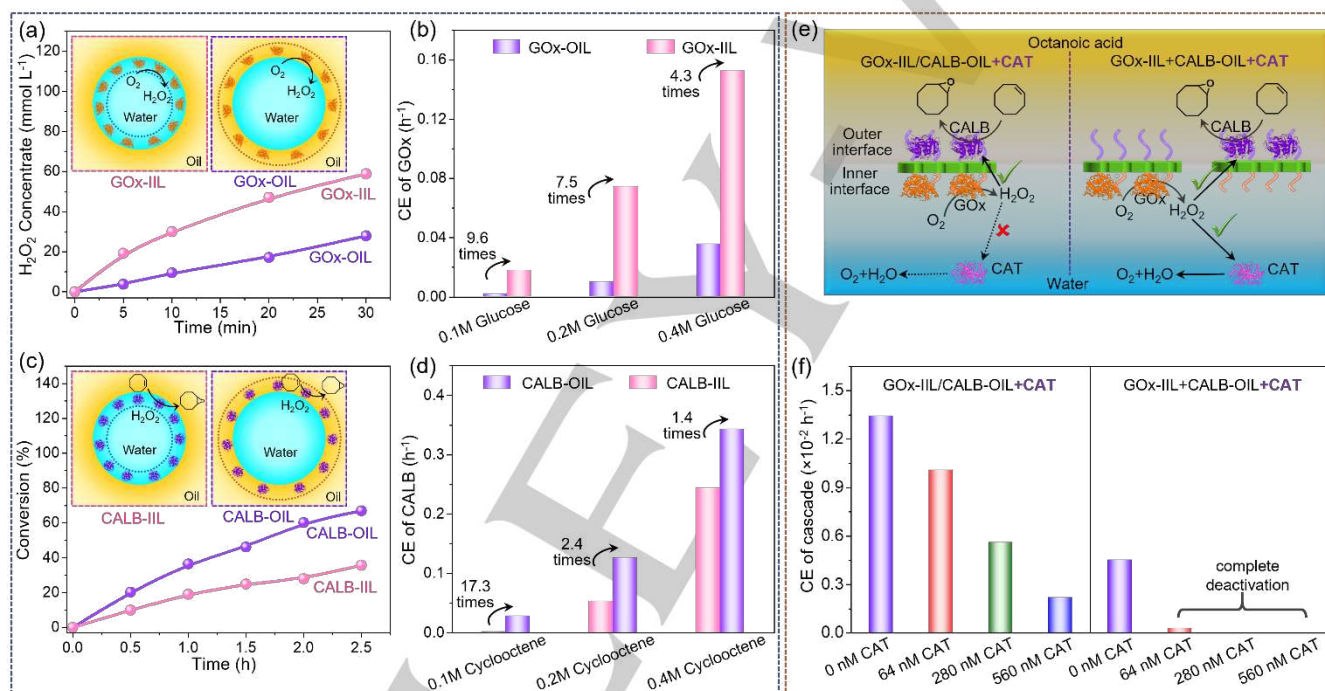


Figure 4. Interfacial effect. (a) Kinetic profiles for the production of H₂O₂ from glucose (0.4M) and molecular oxygen over GOx-IIL and GOx-OIL. Insets: Schematic illustrations for the GOx enzyme located in the inner interfacial layer of Pickering droplets (GOx-IIL) and in the outer interfacial layer of Pickering droplets (GOx-OIL). (b) Catalytic efficiencies (CE) of GOx-IIL and GOx-OIL for producing H₂O₂ under different concentrations of glucose. (c) Kinetic profiles for the epoxidation of cyclooctene (0.2M) in the presence of H₂O₂ over CALB-IIL and CALB-OIL. Insets: Schematic illustrations for the CALB enzyme located in the inner interfacial layer of Pickering droplets (CALB-IIL) and in the outer interfacial layer of Pickering droplets (CALB-OIL). (d) Catalytic efficiencies (CE) of CALB-IIL and CALB-OIL for the cyclooctene epoxidation under different concentrations of cyclooctene. (e) Schematic illustration for the GOx-IIL/CALB-OIL and GOx-IIL+CALB-OIL cascade with a competitive reaction of H₂O₂ decomposition over CAT inside Pickering droplets for the cyclooctene epoxidation. (f) Catalytic efficiencies (CE) of the GOx-IIL/CALB-OIL and GOx-IIL+CALB-OIL cascade for the cyclooctene epoxidation in the presence of different concentrations of CAT.

Origin of the Enhanced Cascading Efficiency

To understand the role of reaction microenvironment in interfacial biocatalytic cascades, the impact of the position of enzymes at the Pickering droplet interfaces on their activities in the single step reaction was investigated. GOx was separately placed in either the inner or the outer interfacial layers of Pickering droplets (Figures S12 and S15), which was achieved by immobilizing it on different surfaces of JMSNs (see the Experimental Section in the Supporting Information). As displayed in Figure 4a, the GOx located in the inner interfacial layer of Pickering droplets (GOx-

IIL) had a faster reaction rate than that residing in the outer interfacial layer (GOx-OIL) in the production of H₂O₂. The catalytic efficiency of GOx-IIL was calculated to be 4.3-times higher than that of GOx-OIL (Figure 4b). These differences suggested that GOx preferred hydrophilic reaction microenvironments for producing H₂O₂, which was likely caused by the higher affinity to the hydrophilic substrate (glucose).^[14] To validate this hypothesis, we further inspected the influence of the glucose concentrations on the catalytic behaviors of both GOx-IIL and GOx-OIL. As displayed in Figure S16, GOx-IIL always presents a higher

RESEARCH ARTICLE

reaction rate than GOx-OIL under all the glucose concentrations. Interestingly, the activity enhancement was observed to be much more pronounced with a decreasing concentration of glucose from 0.4 to 0.1 mol/L (Figure 4b). Under low glucose concentration (0.1 mol/L), GOx-IIL even showed a 9.6-times enhancement in catalytic efficiency in comparison to GOx-OIL. These results confirmed that GOx located in hydrophilic reaction microenvironments possessed a higher affinity to the substrate and thus presented a substantially higher catalytic activity for the production of H₂O₂.

Likewise, CALB was introduced into different interfacial regions of Pickering droplets via the same methods (Figures S12 and S17) and was evaluated in the epoxidation of cyclooctene in the presence of H₂O₂ (the second step reaction). In contrast to the first step reaction, for this second step, CALB located in the outer interfacial layer of Pickering droplets (CALB-OIL) exhibited a 2.4-fold higher catalytic efficiency (Figures 4c, d) in comparison to that in the inner interfacial layer (CALB-IIL). In the presence of a low concentration of alkene, an even higher 17.3-fold activity enhancement was observed (Figure 4d and Figure S18). This finding illustrated that CALB located in hydrophobic reaction microenvironments had a higher affinity to the hydrophobic substrate (alkene) and thereby presented a higher catalytic efficiency for the alkene epoxidation. These results demonstrated that the Pickering droplet interfaces could concurrently provide a preferred reaction medium for both enzymes, so as to ensure the enzymatic reaction networks avoiding mutual interferences.

Furthermore, we noticed that the activity of CALB was sensitive to the local concentration of H₂O₂ in the epoxidation reaction (Figure S19), and then the transportation of the *in-situ* produced H₂O₂ from GOx to CALB was examined to unravel the impact of the inter-enzyme distance on the interfacial biocatalytic cascades. Catalase (CAT) is an exclusive enzyme for the decomposition of H₂O₂ to O₂ and H₂O and it could be used to inspect the proximity effect in multi-enzymatic reactions through introducing a competing reaction.^[15] Thereupon, CAT with varying concentrations were introduced into the internal water phase of Pickering droplets for examining the transfer of H₂O₂ from GOx to CALB (Figure 4e). As shown in the reaction kinetics (Figure S20a), the interfacial GOx-IIL/CALB-OIL cascade still gave a conversion of 73.2% with an epoxide selectivity of 100% within 10.0 h in the presence of 64 nM of CAT that was consuming H₂O₂ with a decomposition rate of 3.2 mM/min. The conversion was only slightly lower than that obtained in the absence of CAT (75.4%). Gradually increasing the concentration of CAT to 280 nM and then further to 560 nM (the decomposition rate of H₂O₂ could reach as high as 28 mM/min), the interfacial GOx-IIL/CALB-OIL cascade retained catalytic efficiencies of 41.7% and 16.4 % (Figure 4f), respectively. In stark contrast, the GOx-IIL+CALB-OIL cascade with a microscale GOx-CALB distance was found to be almost completely deactivated when only 64 nM of CAT was introduced inside the Pickering droplets (Figure 4f and Figure S20b). This difference in the loss of catalytic efficiency would have only resulted from distinctly different inter-enzyme distances in these two systems (Figure 4e). For the interfacial GOx-IIL/CALB-OIL cascade, the nanoscale GOx-CALB distance was much smaller than that of GOx-CAT (microscale). Thus the *in-situ* produced H₂O₂ on GOx was still preferentially transferred to CALB, with the competitive CAT inside the droplets not able to exert much influence on the cascading efficiency. However, the microscale GOx-CALB distance of the GOx-IIL+CALB-OIL cascade was

quite comparable to the distance of GOx-CAT and then the *in-situ* produced H₂O₂ diffused to CALB or CAT, significantly lowering the local H₂O₂ concentration of CALB and quenching the epoxidation reaction.

The same concentration of CAT was also added to the reaction system of free enzymes in solution (GOx+CALB-IPD) and the interfacial GOx-IIL/CALB-OIL cascade with a larger GOx-CALB distance (60 nm). It was found that the GOx+CALB-IPD cascade was thoroughly inactive in the presence of only 64 nM of CAT (Figure S21). Because GOx, CALB and CAT were all uniformly mixed in the internal water phase of Pickering droplets in this case (Figure S21a), a similar deactivation process with the GOx-IIL+CALB-OIL cascade was presented. The interfacial GOx-IIL/CALB-OIL-60 cascade could separately maintain 65.0% and 36.4 % of catalytic efficiency when the concentration of CAT was set at 64 nM and 280 nM (Figure S22), respectively. Distinctly, this activity decline was still more pronounced than that obtained by GOx-IIL/CALB-OIL-40. These results validated that the nanoscale inter-enzyme distances greatly boosted the transport of H₂O₂ from GOx to CALB, thus substantially enhancing the catalytic efficiency of the interfacial GOx-IIL/CALB-OIL cascade. Taken together, Pickering droplet interfaces manipulated the enzymatic reaction networks to avoid their mutual interferences and ensure them working effectively through providing preferable reaction microenvironments for different enzymes and simultaneously facilitated reaction intermediates transportation through tuning the inter-enzyme distances. This remarkable interfacial effect was responsible for the significantly enhanced cascading efficiency of the interfacial biocatalytic cascades.

Conclusion

In conclusion, the present study has introduced a novel design of interfacial biocatalytic cascades for chemical transformations by spatially co-localizing two different enzymes at Pickering droplets interfaces. Based on the interfacial assembly of JMSNs, two different enzymes not only were accommodated in their respective preferred reaction microenvironments but also were retained in a nanoscale proximity of each other. Impressively, the obtained interfacial biocatalytic cascades showed an outstanding catalytic efficiency in the alkene epoxidation and the thioether oxidation with *in-situ* produced H₂O₂ under mild conditions, which was 6.9-times and 13.6-times higher than those of the free enzymes in solution and the multi-enzymatic counterparts, respectively. Importantly, it was demonstrated that Pickering droplet interfaces not only provided concurrently preferable reaction microenvironments for multiple enzymes to avoid their mutual interferences but also facilitated reaction intermediates transportation, which has not been achieved in previously reported biocatalytic cascade processes. Such a remarkable interfacial effect thus contributed to the outstanding catalytic efficiency of our interfacial biocatalytic cascades. Our proposed strategy of spatial localization of multiple enzymes at oil-water interfaces along with the unveiled interfacial effects provide an innovative platform to design efficient biocatalytic cascades for the synthesis of fine chemicals.

Acknowledgements

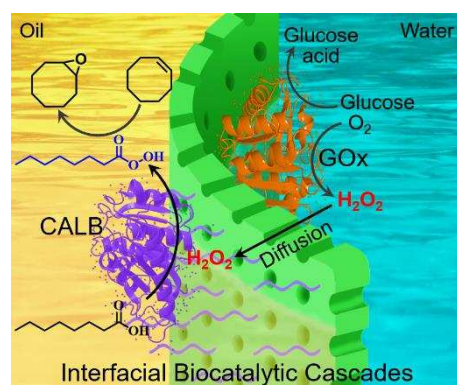
RESEARCH ARTICLE

This work was supported by the National Key Research and Development Program of China (2021YFC2101900), and the National Natural Science Foundation of China (21925203 and 22172094). We are grateful for the test platform provided by the Shanxi University of Scientific Instrument Center.

Keywords: Pickering emulsions • Cascade reactions • Liquid-liquid interfaces • Oxidation • Biocatalysis

- [1] a) F. G. Mutti, T. Knaus, N. S. Scrutton, M. Breuer, N. J. Turner, *Science* **2015**, *349*, 1525–1529; b) M. Vázquez-González, C. Wang, I. Willner, *Nat. Catal.* **2020**, *3*, 256–273; c) A. I. Benítez-Mateos, D. R. Padrosa, F. Paradisi, *Nat. Chem.* **2022**, *14*, 489–499; d) J. H. Schrittwieser, S. Velikogne, M. Hall, W. Kroutil, *Chem. Rev.* **2018**, *118*, 270–348; e) J. Shi, Y. Wu, S. Zhang, Y. Tian, D. Yang, Z. Jiang, *Chem. Soc. Rev.* **2018**, *47*, 4295–4313; f) C. T. Walsh, B. S. Moore, *Angew. Chem. Int. Ed.* **2019**, *58*, 6846–6879.
- [2] a) M. T. Reetz, *J. Am. Chem. Soc.* **2013**, *135*, 12480–12496; b) I. Wheeldon, S. D. Minter, S. Banta, S. C. Barton, P. Atanassov, M. Sigman, *Nat. Chem.* **2016**, *8*, 299; c) A. Küchler, M. Yoshimoto, S. Luginbühl, F. Mavelli, P. Walde, *Nat. Nanotechnol.* **2016**, *11*, 409–420; d) L. Lancaster, W. Abdallah, S. Banta, I. Wheeldon, *Chem. Soc. Rev.* **2018**, *47*, 5177–5186; e) Y. Wang, Q. Zhao, R. Haag, C. Wu, *Angew. Chem. Int. Ed.* **2022**, e202213974.
- [3] a) Z. Zhou, M. Hartmann, *Chem. Soc. Rev.* **2013**, *42*, 3894–3912; b) A. F. Mason, N. A. Yewdall, P. L. W. Welzen, J. Shao, M. van Stevendaal, J. C. M. van Hest, D. S. Williams, L. K. E. A. Abdelmohsen, *ACS Cent. Sci.* **2019**, *5*, 1360–1365; c) C. Wang, L. Yue, I. Willner, *Nat. Catal.* **2020**, *3*, 941–950; d) S. Ren, C. Li, X. Jiao, S. Jia, Y. Jiang, M. Bilal, J. Cui, *Chem. Eng. J.* **2019**, *373*, 1254–1278.
- [4] a) O. I. Wilner, Y. Weizmann, R. Gill, O. Lioubashevski, R. Freeman, I. Willner, *Nat. Nanotechnol.* **2009**, *4*, 249–254; b) J. Fu, M. Liu, Y. Liu, N. W. Woodbury, H. Yan, *J. Am. Chem. Soc.* **2012**, *134*, 5516–5519; c) J. Fu, Y. R. Yang, A. Johnson-Buck, M. Liu, Y. Liu, N. G. Walter, N. W. Woodbury, H. Yan, *Nat. Nanotechnol.* **2014**, *9*, 531–536; d) G. Ke, M. Liu, S. Jiang, X. Qi, Y. R. Yang, S. Wootten, F. Zhang, Z. Zhu, Y. Liu, C. J. Yang, H. Yan, *Angew. Chem. Int. Ed.* **2016**, *55*, 7483–7486.
- [5] a) W. H. Chen, M. Vázquez-González, A. Zoabi, R. Abu-Reziq, I. Willner, *Nat. Catal.* **2018**, *1*, 689–695; b) X. Wu, H. Yue, Y. Zhang, X. Gao, X. Li, L. Wang, Y. Cao, M. Hou, H. An, L. Zhang, S. Li, J. Ma, He Lin, Y. Fu, H. Gu, W. Lou, W. Wei, R. N. Zare, J. Ge, *Nat. Commun.* **2019**, *10*, 5165; c) T. Man, C. Xu, X. Y. Liu, D. Li, C. K. Tsung, H. Pei, Y. Wan, L. Li, *Nat. Commun.* **2022**, *13*, 305; d) Z. Tang, X. Li, L. Tong, H. Yang, J. Wu, X. Zhang, T. Song, S. Huang, F. Zhu, G. Chen, G. Ouyang, *Angew. Chem. Int. Ed.* **2021**, *60*, 23608–23613; e) J. Liang, S. Gao, J. Liu, M. Y. B. Zulkifli, J. Xu, J. Scott, V. Chen, J. Shi, A. Rawal, K. Liang, *Angew. Chem. Int. Ed.* **2021**, *60*, 5421–5428.
- [6] a) M. Li, S. Qiao, Y. Zheng, Y. H. Andaloussi, X. Li, Z. Zhang, A. Li, P. Cheng, S. Ma, Y. Chen, *J. Am. Chem. Soc.* **2022**, *142*, 6675–6681; b) S. Huang, G. Chen, G. Ouyang, *Chem. Soc. Rev.* **2022**, *51*, 6824–6863.
- [7] a) D. Dedovets, Q. Li, L. Leclercq, V. Nardello-Rata, J. Leng, S. Zhao, M. Pera-Titus, *Angew. Chem. Int. Ed.* **2022**, *61*, e202107537; b) L. Ni, C. Yu, Q. Wei, J. Qiu, *Angew. Chem. Int. Ed.* **2022**, *61*, e202115885; c) Z. Wu, L. Li, T. Liao, X. Chen, W. Jiang, W. Luo, J. Yang, Z. Sun, *Nano Today* **2018**, *22*, 62–82; d) L. Leclercq, A. Mouret, A. Proust, V. Schmitt, P. Bauduin, J. M. Aubry, V. Nardello-Rataj, *Chem. Eur. J.* **2012**, *18*, 14352–14358; e) B. Wang, B. Yin, Z. Zhang, Y. Yin, Y. Yang, H. Wang, T. P. Russell, S. Shi, *Angew. Chem. Int. Ed.* **2022**, *61*, e202114936; f) T. Zhao, X. Zhu, C. Hung, P. Wang, A. Elzatahry, A. Al-Khalaf, W. Hozzein, F. Zhang, X. Li, D. Zhao, *J. Am. Chem. Soc.* **2018**, *140*, 10009–10015.
- [8] a) S. Crossley, J. Faria, M. Shen, D. E. Resasco, *Science* **2010**, *327*, 68–72; b) B. Yang, L. Leclercq, V. Schmitt, M. Pera-Titus, V. Nardello-Rataj, *Chem. Sci.* **2019**, *10*, 501–507.
- [9] a) Z. Sun, U. Glebe, H. Charan, A. Böker, C. Wu, *Angew. Chem. Int. Ed.* **2018**, *57*, 13810–13814; b) Z. Sun, R. Hübner, J. Li, C. Wu, *Nat. Commun.* **2022**, *13*, 3142.
- [10] a) H. Tan, S. Guo, N. D. Dinh, R. Luo, L. Jin, C. H. Chen, *Nat. Commun.* **2017**, *8*, 663; b) Y. Chen, M. Yuan, Y. Zhang, S. Liu, X. Yang, K. Wang, J. Liu, *Chem. Sci.* **2020**, *11*, 8617–8625; c) R. Booth, Y. Qiao, M. Li, S. Mann, *Angew. Chem. Int. Ed.* **2019**, *58*, 9120–9124; d) S. Jiang, L. Silva, T. Ivanov, M. Mottola, K. Landfester, *Angew. Chem. Int. Ed.* **2022**, *61*, e202113784; e) W. Wei, R. Ettelaie, X. M. Zhang, M. Fan, Y. Dong, Z. B. Li, H. Q. Yang, *Angew. Chem. Int. Ed.* **2022**, *61*, e202211912.
- [11] a) F. Liang, K. Shen, X. Qu, C. Zhang, Q. Wang, J. Li, J. Liu, Z. Yang, *Angew. Chem. Int. Ed.* **2011**, *50*, 2379–2382; b) S. Yan, H. Zou, S. Chen, N. Xue, H. Yang, *Chem. Commun.* **2018**, *54*, 10455–10458; c) H. Zou, H. Shi, S. Hao, Y. Hao, J. Yang, X. Tian, H. Yang, *J. Am. Chem. Soc.* **2023**, *145*, 2511–2522; d) B. Seo, M. Sung, B. J. Park, J. W. Kim, *Adv. Funct. Mater.* **2022**, *32*, 2110439.
- [12] a) B. P. Binks, P. D. I. Fletcher, *Langmuir* **2001**, *17*, 4708–4710; b) A. Kumar, B. J. Park, F. Tu, D. Lee, *Soft Matter* **2013**, *9*, 6604–6617; c) Y. Hao, S. Hao, Q. Li, X. Liu, H. Zou, H. Yang, *ACS Appl. Mater. Interfaces* **2021**, *13*, 47236–47243.
- [13] a) E. Ankudey, H. Olivo, T. Peeples, *Green Chem.* **2006**, *8*, 923–926; b) F. Tieves, S. Willot, M. van Schie, M. Rauch, S. Younes, W. Zhang, J. Dong, P. de Santos, J. Robbins, B. Bommarius, M. Alcalde, A. Bommarius, F. Hollmann, *Angew. Chem. Int. Ed.* **2019**, *58*, 7873–7877.
- [14] S. Bankar, M. Bule, R. Singhal, L. Ananthanarayan, *Biotechnol. Adv.* **2009**, *27*, 489–501.
- [15] Y. Zhang, S. Tsitkov, H. Hess, *Nat. Commun.* **2016**, *7*, 13982.

Entry for the Table of Contents



Two different enzymes were precisely localized at the inner and outer interfaces of Pickering emulsion droplets with the aid of an asymmetrically modified mesoporous nanosheet. This unique system exhibited significantly enhanced cascading efficiency in challenging oxidation reactions by creating reaction microenvironments appropriate for the different enzymes and enabling efficient intermediate transportation at the droplet interfaces.